Kinematics and Optimization of 2-DOF Parallel Manipulator with Revolute Actuators and a Passive Leg

Yun-Joo Nam
Department of Mechanical and Intelligent Systems Engineering, Pusan National University, 30 Jangjeon-dong, Geumjeong-gu, Busan 609-735, Korea
Myeong-Kwan Park*
Research Institute of Mechanical Technology, School of Mechanical Engineering, Pusan National University, 30 Jangjeon-dong, Geumjeong-gu, Busan 609-735, Korea

In this paper, a 2-DOF planar parallel manipulator with two revolute actuators and one passive constraining leg. The kinematic analysis of the mechanism is analytically performed : the inverse and forward kinematics problems are solved in closed forms, the workspace is derived systematically, and the three kinds of singular configurations are found. The optimal design to determine the geometric parameters and the operating limits of the actuated legs is performed considering the kinematic manipulability and workspace size. These results of the paper show the effectiveness of the presented manipulator.

Key Words : Kinematics, Limited-DOF Mechanism, Optimal Design, Parallel Manipulator

1. Introduction

Recently, the machine tool industry has introduced a new type of machine tools, called parallel kinematic machines, which are based on the kinematic architecture of parallel manipulators (Tsai and Joshi, 2002). The industrial and economical relevance of parallel kinematic machines is continuously growing, and this technology can be considered as a well-established option for many different application fields such as optical devices, semiconductor manufacturing machines, high precision surgical tools, and micro-positioning devices, because the parallel kinematic machines have a number of advantages relative to conventional machine tools, such as a higher stiffness-to-mass ratio, higher speeds, higher accuracy, reduced installation requirements, mechanical simplicity, and high flexibility (Pham and Chen, 2002 ; Liu et al., 2003 ; Callegari and Taranatini, 2003). However, from the application point of view, limited workspace and complicated kinematic analysis due to their closed-loop nature are the two major drawbacks of parallel mechanisms.

To overcome these drawbacks, parallel manipulators with the limited number of degree-of-freedom (DOF) have attracted more and more researchers' attention in the recent robotic literatures (Ji and Wu, 2003 ; Tsai et al., 2003 ; Gregorio and Parenti-Castelli, 2001 ; Wang et al., 2001 ; Liu et al., 2001 ; Tsai, 2000). Such mechanisms can perform successfully many tasks that have so far required fully-DOF mechanisms and can achieve lower device and operation costs due to simplified designs involving few joints and actuators, simpler control system, and higher speed performance. Furthermore, they can offer a larger workspace for the remaining end-effector motions (Huang et al., 2004). For these reasons, the study of the kinematics and design of limited-DOF mechanisms with novel and/or old architecture is very important.

* Corresponding Author,
E-mail : mkpark1@pusan.ac.kr
TEL : +82-51-510-2464; **FAX** : +82-51-514-0685
Department of Mechanical and Intelligent Systems Engineering, Pusan National University, 30 Jangjeon-dong, Geumjeong-gu, Busan 609-735, Korea. (Manuscript **Received** April 9, 2005; **Revised** February 6, 2006)

Of the limited-DOF mechanisms, 2-DOF planar parallel manipulators are an important class of robotic mechanisms that can follow arbitrary planar curves. Because of their usefulness in applications, these mechanisms have attracted the attention of researchers who have investigated their workspace, mobility, and methods for analysis and design (Choi, 2003; Frisoli et al., 1999; Pham and Chen, 2002; Liu et al., 2003; Kong and Gosselin, 2002; Gregorio, 2002). In particular, they have great potential for microminiaturization due to processing technology developed for microsystems, such as flexible and simple joins and microprecision actuators (Romdhane et al., 2002).

Although, in the classical cases of planar and spatial mechanisms, each leg has the same freedoms as whole mechanism, it is conceivable to design a parallel mechanism with redundant legs for constraining motions of the end-effector. These additional legs permit a separation of the function of constraint from that of actuation at a cost of increased mechanical complexity and chances of leg interference. In such a constrained parallel mechanism, different legs impose different constraints, and only their combined constraints leads to the desired end-effector freedoms (Joshi and Tsai, 2002).

In this paper, we present a 2-DOF planar parallel mechanism which consists of two identically actuated legs with 3-DOF and one passive constraining leg with 2-DOF connecting the moving platform and the fixed base. The degree-of-freedom of the mechanism is dependent of the passive leg's connectivity. By this arrangement of the kinematics, the dexterity of the system can be increased compared to fully parallel kinematics, and the stiffness can be improved by increased redundant constraints due to a passive leg. A proposed kinematic structure is characterized by cylindrical motions of the moving platform including one translational motion and one rotational motion with respect to the base. Especially, the significant advantage of the mechanism is its high rotational capability of about $\pm 90°$. After a short description of the related geometry, both inverse and forward kinematics for the mechanism are derived in closed form, and the workspace boundaries are described analytically. Then, by using the Jacobian matrix derived in a symbolic form, the identification of all singular configurations is achieved based on the singularity classification (Gosselin and Angeles, 1990; Ma and Angeles, 1992). Upon such bases, the mechanism's architecture is optimized by using performance indices defined to evaluate the conditioning, manipulability, and workspace size to the mechanical device bulk. These results of this paper can be of great help in the design, application and control of such devices.

2. Manipulator Description

The 2-DOF parallel manipulator studied in this paper is shown in Fig. 1. This manipulator consists of a moving platform, a fixed base and three legs that meet at three distinct points in the moving platform and the fixed base. Two of the three legs, called the actuated leg, have the same kinematic structure. The i-th actuated leg connects the base to the moving platform by an active revolute joint B_i followed by two passive revolute joints, d_i and b_i. The third leg represented by l_c is a passive constraining leg and has architecture different from the other legs, one end of which is fixed perpendicularly at the center C of the moving platform and the other is jointed at the center O of the base by a passive revolute joint followed by a passive prismatic joint. Here, the geometric parameters of the mechanism are $r=|Cb_i|$, $R=|OB_i|$, $l_a=|B_id_i|$, and $l_b=|d_ib_i|$, which designate the moving platform, the base, the lower

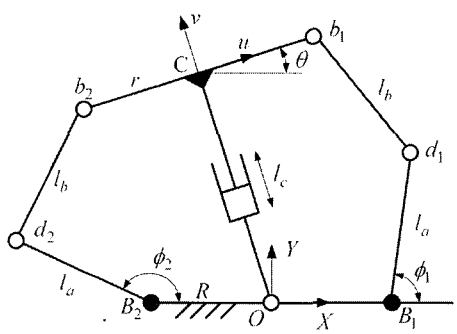

Fig. 1 2-DOF parallel manipulator with a passive constraining leg

link, and the upper link, respectively.

Since the joint degrees of freedom or connectivity of the first two legs are equal to three, these actuated legs do not impose any constraint on the moving platform. In contrary, since the third leg has only two degrees of freedom, it provides one constraint on the moving platform. In other words, the aim of using the passive constraining leg in this manipulator is to eliminate the translation of the moving platform along x axis and to make the actuated legs free from the role of constraining the moving platform. Therefore, this mechanism has 2-DOF including one translation along y axis and one rotation in O_xy plane, which means that the motion of the moving platform is characterized by all possible cylindrical curves within its workspace. Due to the redundant leg and the moving platform but not a point as the end-effector, the proposed manipulator can offer larger workspace, especially wide rotational range, than fully parallel mechanisms, leading to more easy applications of this mechanism to many other machine tools.

2. Position Kinematics

For purpose of kinematic analysis, a fixed reference coordinate frame O_xy is attached to the fixed base at point O and the moving coordinate frame C_uv is attached to the moving platform at point C, as shown in Fig. 1. The x axis of the fixed frame is aligned with the join B_1 while y axis is normal to the fixed base. Similarly, u axis of the moving frame is pointing toward the joint b_1, and v axis is perpendicular to the moving platform.

Let us denote the position and orientation of the moving platform with respect to the base as the coordinate (x_C, y_C) and θ, respectively. Then, the pose of the moving platform with respect to the fixed base can be completely defined by three variables (x_C, y_C, θ). However, since the mechanism is a 2-DOF device, the motion of the moving platform is constrained to lie in a 2-DOF sub-manifold of 3-DOF manifold of general planar motion, which implies that only two variables can be specified independently. For convenience, the independent variables are chosen as (x_C, y_C), and the dependent variable as θ. Considering that the passive constraining leg should be fixed perpendicularly to the moving platform, the relationship between the independent variables and dependent one can be defined by

$$x_C \cos\theta + y_C \sin\theta = 0 \tag{1}$$

where one assumption that $r \neq 0$ is used to design the end-effector in the form of a rigid body, but not a point. From Eq. (1), one can see that the rotation angle θ is the function of the independent variables (x_C, y_C).

3.1 Inverse kinematics

The inverse kinematics is to find a set of input joint variables for a given position and orientation of the moving platform with respect to the base. For the presented parallel manipulator, the output variables (x_C, y_C) are given, and the input joint variables (ϕ_1, ϕ_2) are to be found.

From the geometry of Fig. 1, the closed-loop equations for each actuated leg are written as

$$(x_C + r\cos\theta - R - l_a\cos\phi_1)^2 + (y_C + r\sin\theta - l_a\sin\phi_1)^2 = l_b^2 \tag{2}$$

$$(x_C - r\cos\theta + R - l_a\cos\phi_2)^2 + (y_C - r\sin\theta - l_a\sin\phi_2)^2 = l_b^2 \tag{3}$$

Using the following substitutions in Eqs. (2) and (3)

$$\cos\phi_i = \frac{1-t_i^2}{1+t_i^2} \tag{4}$$

where $t_i = \tan(\phi_i/2)$ for $i=1, 2$, we obtain two 2-order polynomials in t_i as

$$(\gamma_i - \alpha_i)t_i^2 + 2\beta_i t_i + (\gamma_i + \alpha_i) = 0 \tag{5}$$

where

$$\alpha_1 = 2l_a(x_C + r\cos\theta - R)$$

$$\beta_1 = 2l_a(y_C + r\sin\theta)$$

$$\gamma_1 = -(\alpha_1^2 + \beta_1^2)/(4l_a^2) + l_b^2 - l_a^2$$

$$\alpha_2 = 2l_a(x_C - r\cos\theta + R)$$

$$\beta_2 = 2l_a(y_C - r\sin\theta)$$

$$\gamma_2 = -(\alpha_2^2 + \beta_2^2)/(4l_a^2) + l_b^2 - l_a^2$$

Hence, from Eq. (5) and the specified values of the pose of the moving platform, the closed-form solutions to inverse kinematics are obtained as

$$\phi_i=\begin{cases}2\arctan\left(\dfrac{-\beta_i\pm\sqrt{\alpha_i^2+\beta_i^2-\gamma_i^2}}{\gamma_i-\alpha_i}\right) & \text{for } (\gamma_i-\alpha_i)\neq 0\\ -(\gamma_i+\alpha_i)/(2\beta_i) & \text{for } (\gamma_i-\alpha_i)=0\end{cases} \quad (6)$$

from which we can see that there are at most four inverse kinematic solutions for a given pose of the parallel robot. To obtain the configuration as shown in Fig. 1, the sign "±" in Eq. (6) should be "+" for $i=1$ and "−" for $i=2$.

3.2 Forward kinematics

The forward kinematics is to find the position and orientation of the moving platform corresponding to a given set of input joint variables. For the given mechanism, the inputs (ϕ_1, ϕ_2) are known, and the pose of the moving platform (x_C, y_C) are to be found.

First, from Eq. (1) and the architecture of the mechanism, the following relations can be obtained:

$$\begin{cases}x_C=-l_C\sin\theta\\ y_C=l_C\cos\theta\end{cases} \quad (7)$$

where $l_C=(x_C^2+y_C^2)^{1/2}$ is the length of the passive leg. Substituting Eq. (7) into Eqs. (2) and (3) leads to

$$A_i-2B_i\cos\theta+2C_i\sin\theta=0 \text{ for } i=1, 2 \quad (8)$$

where

$$A_1=l_C^2+r^2+R^2+l_a^2-l_b^2+2l_aR\cos\phi_1$$

$$B_1=Rr+l_ar\cos\phi_1+l_Cl_a\sin\phi_1$$

$$C_1=l_CR+l_Cl_a\cos\phi_1-l_ar\sin\phi_1$$

$$A_2=l_C^2+r^2+R^2+l_a^2-l_b^2-2l_aR\cos\phi_2$$

$$B_2=Rr-l_ar\cos\phi_2+l_Cl_a\sin\phi_2$$

$$C_2=-l_CR+l_Cl_a\cos\phi_2+l_ar\sin\phi_2$$

Substituting the trigonometric identity into Eq. (8) and rearranging, we get

$$(A_i-B_i)s^2+2C_is+(A_i+B_i)=0 \quad (9)$$

where $s=\tan(\theta/2)$, $\cos\theta=(1-s^2)/(1+s^2)$, and $\theta=2s/(1+s^2)$. To gain the solution for variable s simultaneously satisfying the above equations, the coefficients of Eq. (9) should meet the following condition:

$$\begin{vmatrix}0 & A_1-B_1 & 2C_1 & A_1+B_1\\ A_1-B_1 & 2C_1 & A_1+B_1 & 0\\ 0 & A_2-B_2 & 2C_2 & A_2+B_2\\ A_2-B_2 & 2C_2 & A_2+B_2 & 0\end{vmatrix}=0 \quad (10)$$

Expanding Eq. (10) and rearranging, we obtain a 6-order polynomial in l_C as

$$(A_1B_2-A_2B_1)^2+(A_2C_1-A_1C_2)^2-(B_2C_1-B_1C_2)^2=0 \quad (11)$$

From Eqs. (7), (8) and (11), we can see that for the given values of (ϕ_1, ϕ_2), there are at most six solutions to the forward kinematics of (x_C, y_C) for the presented manipulator. Note that the actual one of all possible forward configurations can be easily found within milliseconds by using the inverse kinematics with a unique solution.

From the above analysis, we can conclude that a unique solution to inverse kinematics for the 2-DOF mechanism can be obtained and the solution to the forward kinematics can reach at most six, and all solutions to both position kinematics can be found analytically.

4. Workspace Analysis

Workspace is one of significant factors dominating the kinematic performance of a mechanism. For parallel mechanisms, this issue may be more important since they will sometimes have a rather limited workspace.

The workspace of the presented manipulator is the set of all the output variables (x_C, y_C) at which the mechanism can reach. It depends on the geometric constraints due to the mechanism architecture, the limit on the mobility of each actuated leg, and the link interferences (Gregorio, 2002). Here, in order to neglect the mechanical interferences between the links and joints, especially between the passive leg l_C and the base joints B_1 and B_2, the range of the rotation angle of the moving platform is restricted by $\theta=\arctan(-x_C/y_C)\in(-\pi/2, \pi/2)$. Also, the ranges of

motion of the passive revolute joints are given by $\angle d_1 \equiv \angle b_i d_i B_i \in [0, \pi)$ and $\angle b_i \equiv \angle d_i b_i C \in [0, \pi)$ for the avoidance of singular configurations as mentioned in Sec. 5.2.

Considering these mechanical interferences and the singular configurations, we can intuitively determine two boundaries of the workspace, the inner and outer boundaries for given θ, as shown in Fig. 2. The outer boundary is obtained at the configuration which at least one of the actuated legs is perfectly stretched ($\angle d_i = \pi$), and the inner boundary is obtained at configuration which at least one of the actuated legs has its upper link parallel to the moving platform. From the geometric viewpoint of the mechanism, the length of the passive leg at these configurations is given by

$$l_{CM}(\theta) = -R\,\mathrm{sgn}(\theta)\sin\theta + \sqrt{R^2\sin^2\theta - R^2 - r^2 + 2rR\cos\theta + (l_a + l_b)^2} \quad (12)$$

$$l_{Cm}(\theta) = R\,\mathrm{sgn}(\theta)\sin\theta + \sqrt{R^2\sin^2\theta - R^2 - (r + l_b)^2 + 2(r + l_b)R\cos\theta + l_a^2} \quad (13)$$

where $\mathrm{sgn}(\theta)$ is the sign function, and l_{CM} and l_{Cm} represent the maximum and minimum passive leg length obtained at the given θ, respectively. For any $\theta \in (-\pi/2, \pi/2)$, the condition for the existence of a real value for l_{CM} satisfying Eq. (12) is obtained from

$$R^2\sin^2\theta - R^2 - r^2 + 2rR\cos\theta + (l_a + l_b)^2 \geq 0 \iff l_a + l_b > \max\{r, R - r\} \quad (14)$$

Contrary to l_{CM}, we prefer l_{Cm} not to have any real value satisfying Eq. (13) for $\theta \in (-\pi/2, \pi/2)$, because obtaining some real value for l_{Cm} implies that the size of the workspace is reduced due to the inner boundary. Therefore, the condition for imaginary value of l_{Cm} should always be reached :

$$R^2\sin^2\theta - R^2 - (r + l_b)^2 + 2(r + l_b)R\cos\theta + l_a^2 < 0 \iff l_b - l_a \geq R - r \quad (15)$$

Note that the mechanism configuration obtained at the case that $l_b - l_a = R - r$ corresponds to the architecture singular configuration occurred only when the reference point (x_C, y_C) of the moving platform is located at the origin O on the base, as discussed later. Furthermore, since the inequality $l_b - l_a > R - r$ in Eq. (15) makes the singularity of the mechanism exist within the workspace as usual, the relation $l_b - l_a = R - r$ is just considered at the optimal design stage for the largest workspace.

From these analyses, the mechanism designed under the condition of Eq. (14) and $l_b - l_a = R - r$ can achieve the maximum size of its workspace, and the workspace boundary systematically described by Eq. (12) helps one to obtain more accurate performance indices in the stage of the optimal design.

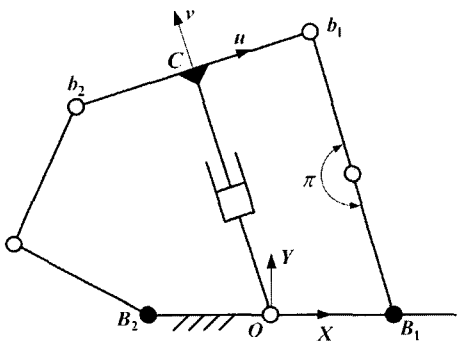

(a) Configuration on the outer boundary and inverse singular configuration

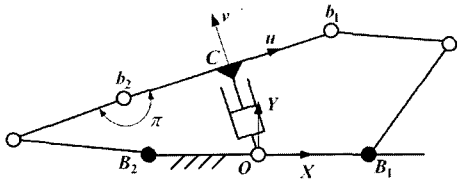

(b) Configuration on inner boundary

Fig. 2 Geometric algorithm for generating the boundary of workspace

5. Jacobian Analysis

In this section, we develop the Jacobian matrix that provides a transformation from the velocity of the moving platform in Cartesian space to the actuated leg velocities in the joint space. The Jacobian is then used to investigate kinematic conditions that lead to singular configurations where the mobility of the manipulator instantaneously changes.

5.1 Jacobian matrices

Differentiating Eqs. (2) and (3) with respect to time, one obtains the velocity equations as

$$X_i\dot{x}_C+Y_i\dot{y}_C+r(-X_i\sin\theta+Y_i\cos\theta)\dot{\theta} = l_a(-X_i\sin\phi_i+Y_i\cos\phi_i)\dot{\phi}_1 \text{ for } =1,\ 2 \tag{16}$$

where

$$X_1=x_C+r\cos\theta-R-l_a\cos\phi_1$$

$$Y_1=y_C+r\sin\theta-l_a\sin\phi_1$$

$$X_2=x_C-r\cos\theta+R-l_a\cos\phi_2$$

$$Y_2=y_C-r\sin\theta-l_a\sin\phi_2$$

Note that $\overline{d_ib_i}=[X_i,\ Y_i]^T$ $(i=1, 2)$ represent the upper links of the actuated legs in vector form, respectively. In order to describe the relationship between the actuated joint velocities $(\dot{\phi}, \dot{\phi}_2)$ and the velocities of the moving platform $(\dot{x}_C, \dot{y}_C)$, the angular velocity $\dot{\theta}$ should be expressed as the function of $\dot{x}_C$ and $\dot{y}_C$, which can be obtained by differentiating Eq. (1) with respect to time as follows

$$\dot{\theta}=\frac{\dot{x}_C\cos\theta+\dot{y}_C\sin\theta}{x_C\sin\theta-y_C\cos\theta} \tag{17}$$

where $x_C\sin\theta-y_C\cos\theta\neq0$, since $x_C\sin\theta-y_C\cos\theta=0$ implies the passive leg length $l_C=0$ which cannot be achieved in practice. Substituting Eq. (17) into Eq. (16) and rearranging in vector form lead to

$$\mathbf{J}_q\dot{\mathbf{q}}=\mathbf{J}_x\dot{\mathbf{x}} \tag{18}$$

where the input and output velocity vectors are defined by $\dot{\mathbf{q}}=[\dot{\phi}_1,\ \dot{\phi}_2]^T$ and $\dot{\mathbf{x}}=[\dot{x}_C,\ \dot{y}_C]^T$, respectively. Matrices $\mathbf{J}_q$ and $\mathbf{J}_x\in\Re^2$ are the inverse and forward Jacobian matrices of the mechanism, respectively, and they are expressed by

$$\mathbf{J}_q=diag(l_a(-X_1\sin\phi_1+Y_1\cos\phi_1),\ l_a(-X_2\sin\phi_2+Y_2\cos\phi_2)) \tag{19}$$

$$\mathbf{J}_x=\begin{bmatrix}X_1+Z_1\cos\theta & Y_1+Z_1\sin\theta\\ X_2-Z_2\cos\theta & Y_2-Z_2\sin\theta\end{bmatrix} \tag{20}$$

where

$$Z_i=\frac{r(-X_i\sin\theta+Y_i\cos\theta)}{x_C\sin\theta-y_C\cos\theta} \text{ for } i=1,\ 2$$

Therefore, the Jacobian matrix of the presented mechanism can be written by

$$\mathbf{J}=\mathbf{J}_q^{-1}\mathbf{J}_x \tag{21}$$

5.2 Singularity analysis

Since the identification of singular configurations is an important issue that should be addressed priori to mechanism design stage, the singularity problem of parallel manipulators has been studied by many researchers. In general parallel mechanisms, a classification of singularities (Gosselin and Angeles, 1990) is suitable for the determination of singularities. The distinction can be made between three kinds of singularities which have different physical interpretations. Therefore, singularities of the presented mechanism occur where $\mathbf{J}_q$, $\mathbf{J}_x$, or both become singular.

The first kind of singularity is related to matrix $\mathbf{J}_q$, which means that $\mathbf{J}_q$ becomes singular but $\mathbf{J}_x$ is invertible. This corresponds to configuration in which the moving platform is at or near boundary of its workspace, and hence, the mechanism can resist external forces or moments without exerting any force of the actuated legs by losing one or more mobility of the moving platform. These singularities can be found from the following conditions:

$$\det(\mathbf{J}_q)=0\Rightarrow l_a(-X_i\sin\phi_i+Y_i\cos\phi_i)=0 \text{ for } i=1 \text{ or } 2 \tag{22}$$

For the intuitive analysis, the conditions for the inverse singularity in Eq. (22) can be expanded and rearranged in vector form as follows

$$\begin{bmatrix}X_i\\ Y_i\end{bmatrix}^T\begin{bmatrix}-l_a\sin\phi_i\\ l_a\cos\phi_i\end{bmatrix}=0 \text{ for } i=1 \text{ or } 2 \tag{23}$$

which can be reached only when $\overline{d_ib_i}$ is perpendicular to the normal vector of $\overline{B_id_i}$, since the length of the lower link l_a should be a positive value in practice. From Eq. (23), we can see that the inverse singularity of the presented mechanism is obtained at the configuration which at least one of the actuated legs is perfectly stretched, i.e. $\overline{d_ib_i}\,//\,\overline{B_id_i}$, as shown in Fig. 2(a).

The second kind of singularity occurs when $\mathbf{J}_q$ is invertible but $\mathbf{J}_x$ becomes singular. This corresponds to configuration in which the moving

platform can move even when all the actuators are locked. In order words, the mechanism gains one degree of freedom such that it cannot resist an external force or moment. From Eq. (20), we can obtain

$$\Rightarrow -2l_C(X_1Y_2-X_2Y_1) +2r(X_1\sin\theta-Y_1\cos\theta)(X_2\sin\theta-Y_2\cos\theta)=0 \quad (24)$$

Note that, from the geometric configuration as shown in Fig. 1, the following inequalities is always reached :

$$\begin{cases} X_1Y_2-X_2Y_1\le 0 \\ X_i\sin\theta-Y_i\cos\theta\le 0 \end{cases} \quad (25)$$

Furthermore, since l_C and r are positive values in practice, Eq. (24) can be expressed as

$$X_1Y_2-X_2Y_1=0 \text{ and } X_i\sin\theta-Y_i\cos\theta=0 \text{ for } i=1 \text{ or } 2 \quad (26)$$

which implies that at least one of the upper links $\overline{d_ib_i}$ is perpendicular to the passive constraining leg l_C and the two upper links are also parallel to each other. Therefore, from Eq. (26), we can see that the forward singularity of the presented mechanism is obtained at the configuration which all upper links of the actuated legs are parallel to the moving platform, i.e. $\overline{d_ib_i}\,//\,\overline{Cb_i}$, as shown in Fig. 3(a).

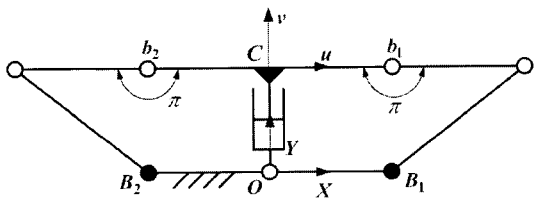

(a) Forward singular configuration

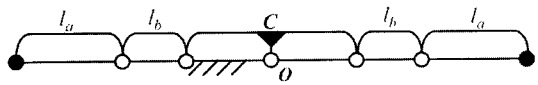

(b) Architecture singular configuration in $R-r=l_a+l_b$

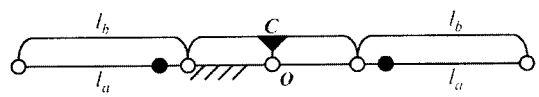

(c) Architecture singular configuration in $R-r=l_b-l_a$

Fig. 3 Singular configurations

The third kind of singularity, called architecture singularity (Ma and Angeles, 1992), occurs when both $\mathbf{J}_q$ and $\mathbf{J}_x$ become simultaneously singular. This corresponds to configurations at which the moving platform can locally move when all the actuators are locked or at which a finite motion of the actuators produces no motion of the mechanism. For such a configuration, the upper link in each actuated leg should be simultaneously parallel to its lower link and the moving platform, as shown in Fig. 3(b) and 3(c). In order that the mechanism performs desired motions as the manipulator, the configuration in Fig. 3(b) is excluded at the mechanical design stage, while the configuration in Fig. 3(c) may be preferred for the largest workspace size as mentioned above. In other words, considering that the outer boundary of the workspace corresponds to the inverse singularity loci and the inner boundary includes the forward singularity at the origin, the architecture singularity point given by $R-r=l_b-l_a$ is a unique choice for the avoidance of the singularity existing within the workspace. Furthermore, the third singularity is just located at the origin O, which leads to the inner boundary of the workspace corresponding to x-axis.

From the above analysis, we can conclude that the well-designed mechanism under the condition $R-r=l_b-l_a$ can be free from the singularity problem by limiting the workspace boundaries to the vicinity of both the inverse singularity loci and the origin.

6. Optimal Design

In general, parallel manipulators have a relatively small workspace. Hence, the workspace size of such manipulators should be maximized. However, a manipulator designed for a maximum workspace may lead to undesirable kinematic characteristics such as poor dexterity or manipulability. Therefore, the quality of workspace should be adequately considered while optimizing it (Stock and Miller, 2003).

It is the aim of this section to determine the dimensions of the geometric parameters and the operating range of the actuated joint for the pre-

sented manipulator through an acceptable compromise between manipulability and workspace size.

6.1 Performance indices

6.1.1 Global conditioning index

The first performance index used in this paper as an objective function for maximization is the global conditioning index (Gao et al., 1998; Frisoli et al., 1999, Liu et al., 2003, Birglen et al., 2002) defined by

$$\eta_1=\frac{\int_W 1/\kappa\, dW}{\int_W dW} \tag{27}$$

where dW is a differential workspace of the manipulator and κ is the condition number of the Jacobian matrix at a given position in the workspace. The workspace W is calculated from Eq. (12) as

$$W=\int_W dW=\int_{-\varphi}^{\varphi} l_{CM}(\theta)\, d\theta \tag{28}$$

where φ represents the positive angle smaller than $\pi/2$, but in the vicinity of $\pi/2$. This index meaning the average value $1/\kappa$ over the workspace is used to evaluate how uniformly the moving platform can move in arbitrary direction within the workspace. Furthermore, the index is independent of workspace sizes varying according to considered mechanisms, since it is normalized by the workspace size.

6.1.2 Global manipulability index

This index representing how fast the moving platform can move in arbitrary direction is defined from the velocity manipulability measure $\bar{\omega}=|\det(\mathbf{J})|$ (Yoshikawa, 1985; 1991) as follows

$$\eta_2=\frac{\int_W \bar{\omega} dW}{\int_W dW} \tag{29}$$

To analyze the manipulability of the mechanism, the manipulability ellipsoid is the most intuitive and useful measure. The manipulability ellipsoid can be made by mapping a unit sphere in the input space of the actuators to the Cartesian space of the moving platform through the Jacobian matrix (Yoshikawa, 1991). This index can be considered as the average value of $\bar{\omega}$ related to the volume of the manipulability ellipsoid over the workspace. Therefore, the larger the global manipulability index is, the greater the total output (velocity) for a given input is.

6.1.3 Space utilization index

This performance index is used to overcome the shortcomings involved in the first two performance indices. Due to the normalizing process for making the performance index independent of the workspace size, the above indices do not adequately represent the effect of the workspace size of the mechanism. For such a consideration, the third index, called the space utilization index, is defined as

$$\eta_3=\frac{\int_W dW}{S} \tag{30}$$

where $S=(r+R)\sqrt{(l_a+l_b)^2-(R-r)^2}$ denotes the physical size of the mechanism obtained when all actuated leg are perfectly stretched. Therefore, the space utilization index reflects the ratio of the workspace size to the physical size occupied by the mechanism. Similarly to the previous indices, this is independent of the overall scale of each design candidate that it is applied to.

It is clear that a practical optimization of the mechanism studied here would require a design index comprising multiple performance indices mentioned above. Since values of the three performance indices may be distributed in different range to each other, in order to make a meaningful comparison among them as well as to prevent simply cancellations between denominators or numerators during the combination process, each of the three indices should be normalized with respect to its extreme values once more. If the normalized index is represented by the superscript hat ($\hat{}$), then the composed design index for the workspace optimization of the mechanism is defined as

$$\eta=\hat{\eta}_1\times\hat{\eta}_2\times\hat{\eta}_3 \tag{31}$$

Therefore, we can see that the composed design

index η is independent of overall scale of the design candidate to which it is applied and is reasonable for considering various kinematic characteristics of the mechanism.

6.2 Numerical optimization

The objective of optimization is to determine the set of the manipulator design parameters leading to the composed design index to be maximized. The design variables for the mechanism include the lower and upper link lengths of the actuated leg, l_a and l_b, and the sizes of the base and moving platforms, r and R. Without loss of generality, by considering $R-r=l_b-l_a$, we can choose two non-dimensional ratios r/R and l_b/R as the design variables, which implies that optimal design results are applicable to any scale of the mechanism and the variable l_a can be found from the above condition by using the resultant variables.

On the basis of the above analysis, assuming that $R=1$ and the given design parameters vary in their constrained ranges, the kinematic optimization problem of the mechanism can be defined as follows

$$\underset{r,l_b}{Maximize}(\eta) \text{ subject to } r,\ l_b\in[0.5,\ 2] \quad (32)$$

Figures 4~6 show the global conditioning index, the global manipulability index, and the space utilization index with respect to r and l_b, actually r/R and l_b/R, respectively, from which we can see that

(1) The global conditioning index exhibits little variation for r larger than 1.2 and generally increases as l_b increases, while the index is sensitive for relatively small values of r and l_b

(2) The global manipulability index exhibits little variation with respect to r and monotonically increases as l_b increases. Similarly to the conditioning index, its variations are very sensitive for small values of r and l_b.

(3) The space utilization index monotonously increases as l_b increases for the specified r. For l_b less than 1.2, this index increases with respect to r, while for l_b greater than 1.2, the index decreases.

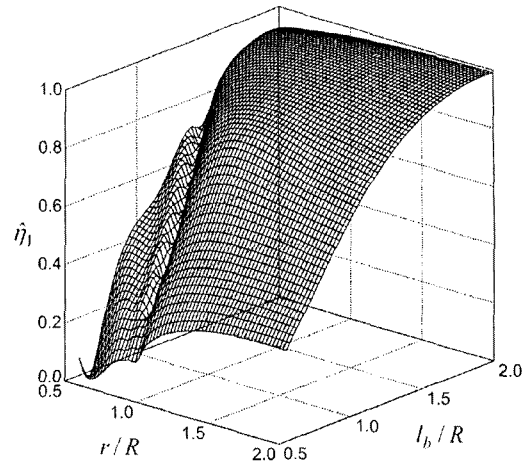

Fig. 4 Normalized global conditioning index

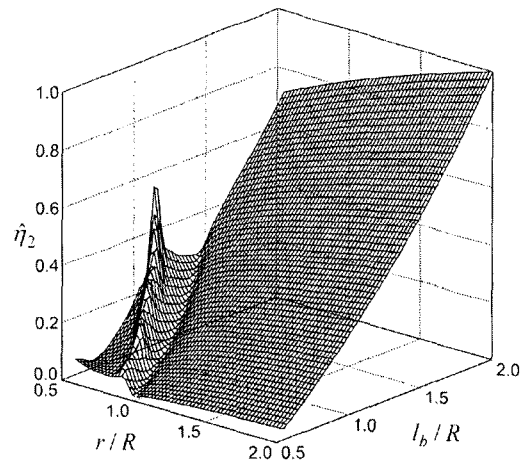

Fig. 5 Normalized global manipulability index

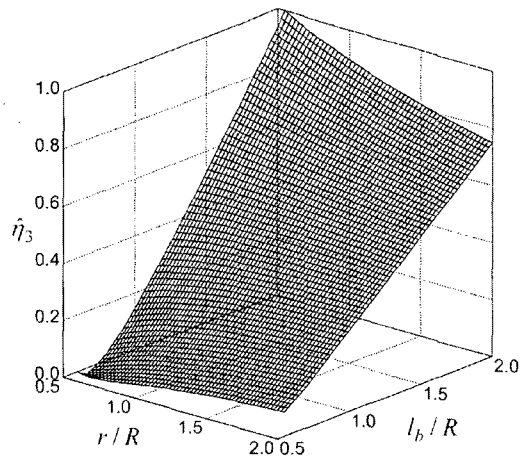

Fig. 6 Normalized space utilization index

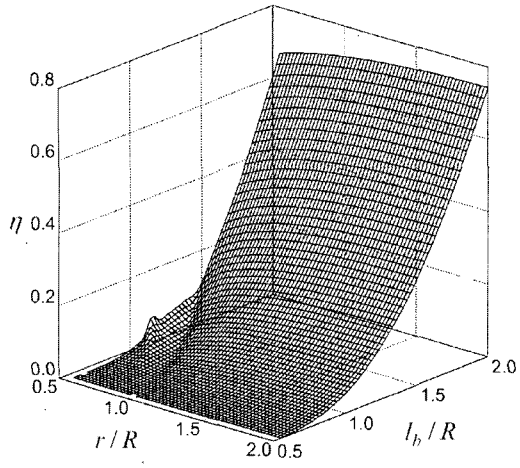

Fig. 7 Composed design index

The result of the composed design index for synthetically considering the effects of three indices is shown in Fig. 7. The composed design index generally increases as l_b increases, while the variation of r has little effect on this index. This means that one can freely select r for the desired characteristic of the mechanism such as dexterity, workspace size.

Now, further studies on the locally kinematic characteristics such as workspace, isotropy, and the operating limits of the actuator are performed with several design variables set. Fig. 8 shows the contours representing the variations of the isotropy $1/\kappa$ within the workspace for three cases of $(r, l_b)=(0.9, 1.2)$, $(1.2, 0.9)$, and $(1.2, 1.2)$. It can be seen that the size of the workspace is more sensitive to l_b compared to r, as expected. The distribution pattern of $1/\kappa$ with respect to the fixed frame O_xy hardly varies according to the variation of l_b, except that the gap of the contours tends to decrease as l_b decreases. Furthermore, by the decrease of r, the contours are distorted around $(x_C, y_C)=(\pm 0.5, 0.5)$. Note that the farther away the reference point on the moving platform is from the origin O, that is, the closer (x_C, y_C) is to the outer boundaries of the workspace, the greater $1/\kappa$ tends to be. From these results, we can see that the presented mechanism has workspace larger than the conventional ones, due to the inner boundary corresponding to x-axis. Also, the mechanism is free from the

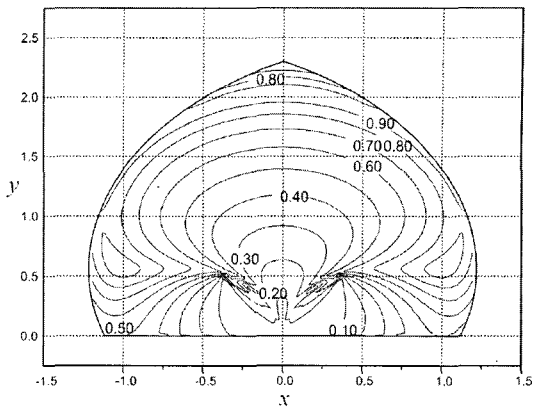

(a) $r=0.9$, $l_b=1.2$

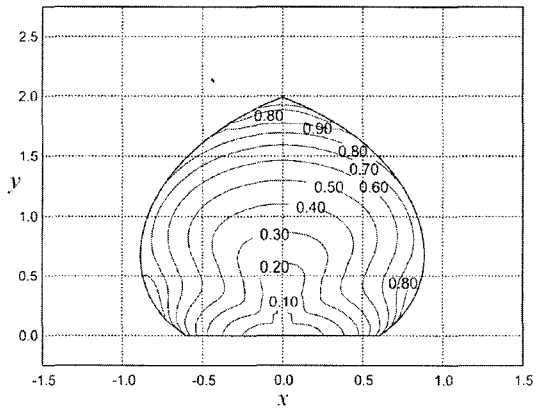

(b) $r=1.2$, $l_b=0.9$

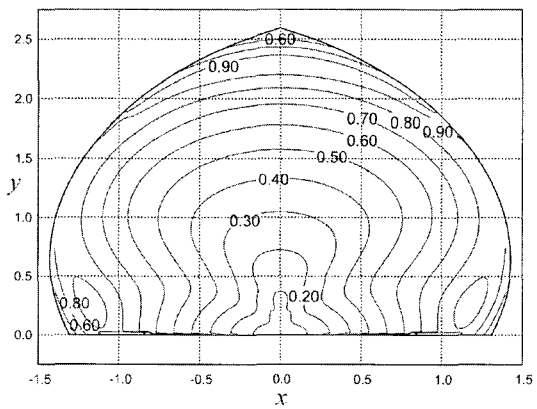

(c) $r=1.2$, $l_b=1.2$

Fig. 8 Contours of $1/\kappa$ in workspace

singularity problem and has favorable isotropy property in the cylindrical area near the outer workspace boundary.

Figure 9 shows the operation limits of the actuators. For $\theta \geq 0$, the maximum rotation angle of ϕ_1 is obtainable at the configuration which the

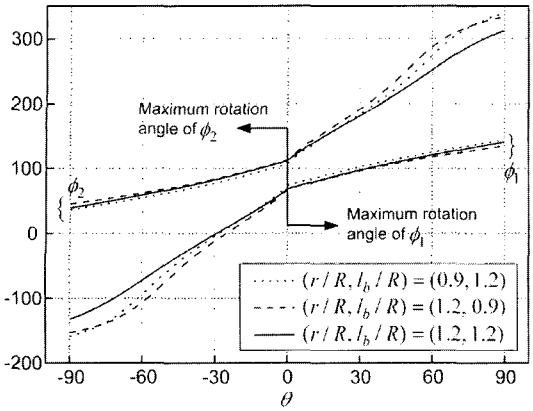

Fig. 9 Operating limits of the actuators according to θ

reference point (x_C, y_C) of the moving platform is located on the outer boundary of the workspace corresponding to the inverse singularity, which means that for the given θ the motion of the mechanism is limited by the first actuator. Similarly, for $\theta \leq 0$ the motion of the mechanism is constrained by the maximum operation limit of the second actuator. This result is very useful index for the real-time control and trajectory planning of this manipulator.

7. Conclustions

A 2-DOF planar parallel manipulator with two actuated leg and one passive constraining leg is presented. The mobility of the presented mechanism is determined to be two freedoms including one translational motion and one rotational motion due to the connectivity of the passive constraining leg, which leads to arbitrary cylindrical motions of the moving platform. First, the kinematic analysis for the manipulator is performed : the closed-form solutions for both the inverse and forward kinematics are found, the boundary of the workspace is derived systematically by using geometrical characteristics of the mechanism, and the all possible singular configurations are found based on the analytically derived Jacobian and a classification of the singularity. Next, the optimal design for the manipulator is performed to determine the dimensions of the geometric parameters with the help of three performance indices defined to effectively represent the globally kinematic performance of the mechanism, such as the conditioning, velocity manipulability, and space utilization. The local performances of the optimized mechanism including the range of the actuated joint variables, kinematic isotropy, and the effects of the design variables on the workspace size are also analyzed. The results of this paper show that the presented manipulator has advantages of high stiffness, high dexterity, high speed, and wide workspace resulting from large rotation capability. Therefore, the manipulator can be effectively used for many applications such as parallel machine tools, precise positioning systems and micromanipulators.

References

Birglen, L., Gosselin, C., Pouliot, N., Monsarrat, B. and Laliberte, T., 2002, "SHaDe, a New 3-DOF Haptic Device," *IEEE Trans. Robot. Automat.*, Vol. 18, No. 2, pp. 166~175.

Callegari, M. and Tarantini, M., 2003, "Kinematic Analysis of a Novel Translational Platform," *Tran. ASME J. Mech. Des.*, Vol. 125, pp. 308~315.

Choi, K. B., 2003, "Kinematic Analysis and Optimal Design of 3-PPR Planar Parallel Manipulator," *KSME International Journal*, Vol. 17, No. 4, pp. 528~537.

Frisoli, A., Prisco, G. M., Salsedo, F. and Bergamasco, M., 1999, "A Two Degrees-Of-Freedom Planar Haptic Interface with High Kinematic Isotropy," *Proc. IEEE Int. Works. on Robot and Human Interaction*, Pisa, Italy, pp. 297~302.

Gao, F., Liu, X. and Gruver, W. A., 1998, "Performance Evaluation of Two-Degree-Of-Freedom Planar Parallel Robots," *Mech. Mach. Theory*, Vol. 33, No. 6, pp. 661~668.

Gregorio, R. D., 2002, "Analytic Determination of Workspace and Singularities in a Parallel Pointing System," *J. Robot. Syst.*, Vol. 19, No. 1, pp. 37~43.

Gregorio, R. D. and Parenti-Castelli, 2001, "Position Analysis in Analytical Form of the 3 -PSP Mechanism," *Tran. ASME J. Mech. Des.*,

Vol. 123, pp. 51~57.

Gosselin, C. M. and Angeles, J., 1990, "Singularity Analysis of Closed Loop Kinematic Chains," *IEEE Trans. Robot. Automat.*, Vol. 6, pp. 281~290.

Huang, T., Li, M., Li, Z., Chetwynd, D. G. and Whitehouse, D. J., 2004, "Optimal Kinematic Design of 2-DOF Parallel Manipulators with Well-Shaped Workspace Bounded by a Specified Conditioning Index," *IEEE Trans. Robot. Automat.*, Vol. 20, No. 3, pp. 538~543.

Ji, P. and Wu, H., 2003, "Kinematics Analysis of an Offset 3-DOF Translational Parallel Robotic Manipulator," *Robotics and Autonomous Systems*, Vol. 42, pp. 117~123.

Joshi, S. A. and Tsai, L. -W., 2002, "Jacobian Analysis of Limited-DOF Parallel Manipulators," *Tran. ASME J. Mech. Des.*, Vol. 124, pp. 254~258.

Joshi, S. and Tsai, L. -W., 2002, "A Comparison Study of Two 3-DOF Parallel Manipulators : One with Three and the Other with Four Supporting Legs," *Proc. IEEE Int. Conf. on Robotics and Automation*, DC, pp. 3690~3697.

Kong, X. and Gosselin, C. M., 2002, "Generation and Forward Displacement Analysis of RPR-PR-RPR Analytic Planar Parallel Manipulators," *Trans. ASME J. Mech. Des.*, Vol. 124, pp. 294~300.

Liu, X. -J, Wang, J., Gao, F. and Wang, L. -P, 2001, "On the Analysis of a New Spatial Three-Degrees-Of-Freedom Parallel Manipulator," *IEEE Trans. Robot. Automat.*, Vol. 17, No. 6, pp. 959~968.

Liu, X. -J., Tang, X. and Wang, J., 2003, "A Novel 2-DOF Parallel Mechanism Based Design of a New 5-axis Hybrid Machine Tool," *Proc. IEEE Int. Conf. on Robotics and Automation*, Taipei, Taiwan, pp. 3990~3995.

Ma, O. and Angeles, J., 1992, "Architecture Singularities of Platform Manipulator," *Proc. IEEE Int. Conf. on Robotics and Automation*, CA, pp. 1542~1547.

Pham, H. H. and Chen, I. -M., 2002, "Kinematics, Workspace and Static Analysis of 2-DOF Flexure Parallel Mechanism," *7th Int. Conf. on Control, Automation, Robotics and Vision*, Singapore, pp. 968~973.

Romdhane, L., Affi, Z. and Fayet, M., 2002, "Design and Singularity Analysis of a 3-Translational-DOF In-Parallel Manipulator," *Tran. ASME J. Mech. Des.*, Vol. 124, pp. 419~426.

Stock, M. and Miller, K., 2003, "Optimal Kinematic Design of Spatial Parallel Manipulators : Application to Linear Delta Robot," *Tran. ASME J. Mech. Des.*, Vol. 125, pp. 292~301.

Tsai, L. -W., 2000, "Kinematics and Optimization of Spatial 3-UPU Parallel Manipulator," *Tran. ASME J. Mech. Des.*, Vol. 122, pp. 439~446.

Tsai, L. -W. and Joshi, S., 2002, "Kinematic Analysis of 3-DOF Position Mechanisms for Use in Hybrid Kinematic Machines," *Tran. ASME J. Mech. Des.*, Vol. 124, pp. 245~253.

Tsai, M. -S., Shiau, T. -N., Tsai, Y. -J. and Chang, T. -H., 2003, "Direct Kinematic Analysis of a 3-PRS Parallel Mechanism," *Mech. Mach. Theory*, Vol. 38, pp. 71~83.

Wang, J., Tang, X., Duan, G. and Li, J., 2001, "Design Methodology for a Novel Planar Three Degrees of Freedom Parallel Machine Tool," *Proc. IEEE Int. Conf. on Robotics and Automation*, Seoul, Korea, pp. 2448~2453.

Yoshikawa, T., 1991, "Translational and Rotational Manipulability of Robotic Manipulators," *Proc. IEEE Int. Conf. on Industrial Electronics, Control and Instrumentation*, pp. 1170~1175.

Yoshikawa, T., 1985, "Manipulability of Robotic Mechanisms," *Int. J. Robotics Research*, Vol. 4, No. 2, pp. 3~9.

Zhang, D. and Gosselin, C. M., 2002, "Kinetostatic Modeling of Parallel Mechanisms with a Passive Constraining Leg and Revolute Actuators," *Mech. Mach. Theory*, Vol. 37, pp. 599~617.